



**HAL**  
open science

## **Ag/ZrO<sub>2</sub> and Ag/Fe–ZrO<sub>2</sub> catalysts for the low temperature total oxidation of toluene in the presence of water vapor**

Rimeh Ismail, Jihene Arfaoui, Zouhaier Ksibi, Abdelhamid Ghorbel, Gerard Delahay

### ► To cite this version:

Rimeh Ismail, Jihene Arfaoui, Zouhaier Ksibi, Abdelhamid Ghorbel, Gerard Delahay. Ag/ZrO<sub>2</sub> and Ag/Fe–ZrO<sub>2</sub> catalysts for the low temperature total oxidation of toluene in the presence of water vapor. *Transition Metal Chemistry*, 2020, 45 (7), pp.501-509. 10.1007/s11243-020-00402-y . hal-02954522

**HAL Id: hal-02954522**

**<https://hal.science/hal-02954522>**

Submitted on 26 Nov 2020

**HAL** is a multi-disciplinary open access archive for the deposit and dissemination of scientific research documents, whether they are published or not. The documents may come from teaching and research institutions in France or abroad, or from public or private research centers.

L'archive ouverte pluridisciplinaire **HAL**, est destinée au dépôt et à la diffusion de documents scientifiques de niveau recherche, publiés ou non, émanant des établissements d'enseignement et de recherche français ou étrangers, des laboratoires publics ou privés.

# Ag/ZrO<sub>2</sub> and Ag/Fe–ZrO<sub>2</sub> catalysts for the low temperature total oxidation of toluene in the presence of water vapor

Rimeh Ismail<sup>1</sup> · Jihène Arfaoui<sup>1</sup> · Zouhaier Ksibi<sup>1</sup> · Abdelhamid Ghorbel<sup>1</sup> · Gérard Delahay<sup>2</sup>

<sup>1</sup> Laboratoire de Chimie Des Matériaux Et Catalyse, Département de Chimie, Faculté Des Sciences de Tunis, Université Tunis El Manar, Campus Universitaire Farhat Hached d'El Manar, 2092 Tunis, Tunisia

<sup>2</sup> Institut Charles Gerhardt Montpellier, CNRS/ENSCM/UM, Matériaux Avancés Pour La Catalyse Et La Santé, 240 avenue du Professeur Emile Jeanbrau, Montpellier, France

Corresponding author : Rimeh Ismail rimeh.ismail@fst.utm.tn

## Abstract

New mesoporous and well-structured Ag-based catalysts ( $x\text{Ag}/\text{ZrO}_2$  and  $x\text{Ag}/\text{Fe}-\text{ZrO}_2$  with  $x = 2 \text{ wt}\%$ ) have been investigated in the total oxidation of toluene with water vapor. The results showed that the catalytic activity of systems increases, in the 350–550 °C temperature range, following this order:  $\text{ZrO}_2 < \text{Fe}-\text{ZrO}_2 < \text{Ag}/\text{ZrO}_2 \approx \text{Ag}/\text{Fe}-\text{ZrO}_2$ . Nevertheless, it was revealed that  $\text{Ag}/\text{Fe}-\text{ZrO}_2$  is the most active solid for the low temperature total oxidation of toluene (< 350 °C). The highest low temperature activity of this new catalyst can be related to the presence of more reactive surface oxygen, new active redox and acidic sites at  $\text{Ag}/\text{Fe}-\text{ZrO}_2$  surface, most probably generated by the simultaneous presence of Ag and Fe species.

Keywords Aerogel supports ·  $\text{Ag}/\text{ZrO}_2$  ·  $\text{Ag}/\text{Fe}-\text{ZrO}_2$  · Toluene oxidation · Water vapor

## Introduction

Volatile organic compounds (VOCs), like aldehydes, alcohols, ketones, aromatic, halogenated and sulfur containing compounds, which can be emitted from automobile industries, petroleum refineries, textile manufacturers, chemical industries, solvents processes, fuel combustions, pharmaceutical plants, decomposition in the biosphere and biomass, etc., remain one of the major sources of air pollution [1, 2]. Therefore, it is necessary to control and reduce the emissions of these compounds. Destructive methods (catalysis oxidation and biofiltration) and recovery methods (condensation, adsorption, absorption, and membrane separation) have been developed for VOCs removal [3]. Among the available technologies, the catalytic oxidation is most popular and effective because of its versatility of eliminating a range of organic pollutants under mild operating conditions [1]. On the other hand, this technique is relatively more environmentally friendly due to its low temperature operation and the formation of less dioxins and noxious products [1]. Divers catalytic systems containing noble or transition metals (e.g., Pd, Pt, Mn, Fe, etc.) have been investigated and demonstrated a high catalytic performances for the destruction of various VOCs (e.g., propane, carbon monoxide, methane, toluene, etc.) [1–11].

In recent years, silver-based materials have been extensively investigated and recognized as suitable catalysts for the low temperatures oxidation of VOCs [6, 12]. These catalysts bring about a special interest due to a number of valuable features of Ag including its ability to activate molecular oxygen, homogeneous distribution of metal particles/clusters over various supports [e.g.,  $\text{TiO}_2$ ,  $\text{ZrO}_2$ ,  $\text{SiO}_2$ ,  $\text{CeO}_2$ ,  $\text{Mn}_x\text{O}_y$ ,  $\text{Si}_3\text{N}_4$ ,  $\text{Fe}_2\text{O}_3$ , etc.] and a synergistic action

with a large number of promoters and modifiers (noble and transition metals, halogen-containing compounds, etc.) [12]. Recently, the activity exploration focused on various Ag supported catalysts has attracted increasing interest in the oxidation of toluene which is known as one of the most targeted components among VOCs [6, 13, 14]. In this framework, Qu et al. [13] have showed that the addition of Ag greatly enhances the reactivity of Mn/SBA-15 for toluene oxidation. The authors have reported that the strong interactions between Ag and Mn species promotes both the reducibility of catalysts and the formation of abundant active lattice oxygen, thus increasing the catalytic activity. On the other hand, Zhang et al. [6] have studied the effect of Ag loading on the structure and performance of the Ag nanoparticles supported on UiO-66 catalysts for toluene oxidation. They have concluded that the increase of the Ag amount affects the UiO-66 structure and the 10Ag-U catalyst showed excellent catalytic performance due to higher lattice oxygen and surface Ag<sup>0</sup> content. Furthermore, Lu et al. [14] have studied the removal of toluene by plasma-catalytic oxidation (non-thermal plasma (NTP)) over Ag-modified FeO<sub>x</sub> / SBA-15 solids. Their results revealed that the incorporation of FeO<sub>x</sub> and AgO<sub>x</sub> significantly enhances the toluene removal efficiency and CO<sub>2</sub> selectivity of the NTP systems. The authors have reported that the silver particles tended to cover the catalyst surface in the form of Ag and Ag<sub>2</sub>O, which improves the dispersion of FeO<sub>x</sub> and lengthened the residual time of toluene in the NTP-catalytic system, thereby promoting the reaction of toluene with oxygen on the catalyst surface increasing toluene oxidation and catalyst stability.

To the best of our knowledge, up to date, no studies related to the total oxidation of toluene (C<sub>6</sub>H<sub>5</sub>-CH<sub>3</sub>) over Ag and Fe supported on ZrO<sub>2</sub> solid, has been described in the literature. Therefore, we reported in this work the preparation and characterization of new Ag/ZrO<sub>2</sub>, Fe-ZrO<sub>2</sub>, and Ag/Fe-ZrO<sub>2</sub> catalytic systems for the total oxidation of toluene in the presence of water vapor. ZrO<sub>2</sub> and Fe-ZrO<sub>2</sub> catalytic supports were prepared by the one step sol-gel procedure which represent one of the low cost techniques that can easily be applied to large area deposition [15, 16]. This method allows the facile synthesis of stable metal oxides with better purity and homogeneity at ambient conditions [15]. It gives high chemical homogeneity, provides good dispersion nanoparticles, well-controlled composition, and useful for the applications where large area coatings are required [15]. Silver was deposited at ZrO<sub>2</sub> and Fe-ZrO<sub>2</sub> surface by the impregnation method. The mutual relationship between the physicochemical properties and catalytic activity in the toluene oxidation of Ag/ZrO<sub>2</sub>, Fe-ZrO<sub>2</sub>, and Ag/Fe-ZrO<sub>2</sub> samples has been discussed.

## Experimental

### Catalysts preparation

ZrO<sub>2</sub> and Fe-ZrO<sub>2</sub> aerogel supports were prepared by the sol-gel method using a similar procedure to that reported in our previous work for TiO<sub>2</sub> [17]. In fact, the requisite quantities of Zirconium (IV) butoxide (Zr(OC<sub>4</sub>H<sub>9</sub>)<sub>4</sub>, Sigmaaldrich, Purity (p) = 80 %) and Ethyl acetoacetate (C<sub>6</sub>H<sub>10</sub>O<sub>3</sub>, Fluka, Purity (p) > 99.5% Sigma-aldrich, p = 80%) were dissolved in anhydrous ethanol (C<sub>2</sub>H<sub>6</sub>O, Aldrich, p = 99.8%) and mixed under stirring at room temperature. Then, a dilute solution of HNO<sub>3</sub> (0.1 M) was gradually added with a suitable molar ratio nH<sub>2</sub>O/nZr = 10 to control hydrolysis. Finally, the mixture was kept under continuous stirring at

room temperature until gelification. For Fe-ZrO<sub>2</sub> solid, an appropriate amount of iron(III) nitrate (Fe(NO<sub>3</sub>)<sub>3</sub>·6H<sub>2</sub>O), Sigma-aldrich, p ≥ 99.95%) was introduced in the mixture before hydrolysis. The resulting gel were dried in autoclave (at T = 243 °C and P = 63 bar) to form the aerogel supports (ZrO<sub>2</sub>, Fe-ZrO<sub>2</sub>) which were calcined at 550 °C for 3 h under O<sub>2</sub> flow (30 cm<sup>3</sup>/min). The Ag/ZrO<sub>2</sub> and Ag/Fe-ZrO<sub>2</sub> catalysts, containing a theoretical loading 2 wt% of Ag, were prepared by the

standard impregnation method. Hence, the required quantity of AgNO<sub>3</sub> (Sigma-Aldrich, p ≥ 99.0% was dissolved in water (H<sub>2</sub>O) and the obtained clear solution was mixed under stirring with ZrO<sub>2</sub> or Fe–ZrO<sub>2</sub> powder to obtain Ag/ZrO<sub>2</sub> or Ag/Fe–ZrO<sub>2</sub> sample which was dried at 100 °C for 12 h and subsequently calcined at 550 °C for 3 h under O<sub>2</sub> flow (30 cm<sup>3</sup> /min).

### Catalytic tests

The toluene oxidation tests were carried out in a fixed bed reactor using 20 mg of catalyst which was packed between the layers of a quartz wool. The catalyst bed temperature was monitored and controlled by a temperature controller equipped with two thermocouples inserted at the catalyst reactor bed and furnace. The toluene concentration was adjusted by passing an appropriate He flow through a saturator, kept at 0.7 °C, containing toluene. A total flow rate of 50 cm<sup>3</sup> /min gas mixture containing 0.1 vol% toluene (purity; p > 99.7%), 3.4 vol% H<sub>2</sub> O (p > 99.5%), 8 vol% O<sub>2</sub> (p > 99.9%) and balance with He (p > 99.9%) were used. The equivalent gas hourly space velocity (GHSV) obtained was of 60,000 h<sup>-1</sup>. The catalytic activity was evaluated in terms of toluene conversion to CO<sub>2</sub>, in the 200–550 °C temperature range, with a ramp of 6 °C/min. Exit gases were monitored continuously by sampling on line to a quadrupole mass gas spectrometer Pfeiffer Vacuum equipped with Faraday and SEM detectors (0–200 amu).

The toluene conversion (%) is expressed as:

$$X_{\text{tot}}(\%) = \frac{[\text{Toluene}]_{\text{in}} - [\text{Toluene}]_{\text{out}}}{[\text{Toluene}]_{\text{in}}} * 100,$$

where [Toluene]<sub>in</sub> and [Toluene]<sub>out</sub> are the inlet and outlet concentrations of toluene, respectively.

The concentration of CO<sub>2</sub> (ppm) was calculated as given below:

$$[\text{CO}_2](\text{ppm}) = \frac{[I]_t - [I]_0}{[I]_{7000}} * 7000,$$

where [I]<sub>0</sub>, [I]<sub>7000</sub> and [I]<sub>t</sub> are the intensity of CO<sub>2</sub> signals at inlet, outlet and at any reaction temperature (t), respectively. 7000 ppm is the inlet concentration of CO<sub>2</sub>.

### Catalysts characterization

Textural properties of the samples were determined by N<sub>2</sub>-physisorption at 77 K using a Micromeritics ASAP 2000 instrument. The samples were previously degassed for 5 h at 250 °C. Structural features were investigated by a Brüker AXS D8 diffractometer with CuKα radiation (λ = 1.5406 Å) and the spectra were collected using a step size of 0.02° in the range 20° and 70°. JCPDS powder diffraction files were used for phase identification. Redox behaviors of solids were analyzed by temperature-programmed reduction technique (H<sub>2</sub>-TPR) with an AUTOCHEM 2910 (Micromeritics). Prior to H<sub>2</sub>-TPR measurements, the sample (80 mg) was pre-treated under 5 vol% O<sub>2</sub> in He (30 cm<sup>3</sup>/min) at 550 °C (ramp 10 °C min<sup>-1</sup>) for 30 min. After being cooled down to 50 °C in the same atmosphere, the sample was flushed with He (30 cm<sup>3</sup>/min) then exposed to a flow containing 5 vol% H<sub>2</sub> in Ar (30 cm<sup>3</sup>/min) and heated between 50 °C and 800 °C with a heating rate of 10°C/min. Acidity of samples was examined by NH<sub>3</sub>-TPD using an AUTOCHEM 2910 (Micromeritics). The solid was pre-treated at 550 °C (ramp 10 °C/min) during 2 h, under air flow (30 cm<sup>3</sup>/min). Then, it was exposed to 5 vol% NH<sub>3</sub> in He (flow rate = 30 cm<sup>3</sup>/min) for 30 min to be flushed after with He (30 cm<sup>3</sup>/min) during 30 min to remove the physisorbed ammonia. Finally, the NH<sub>3</sub> desorption was

done in helium flow (30 cm<sup>3</sup>/min) from 100 to 550 °C (the heating rate was 10 °C/min).

## Results and discussion

The samples (ZrO<sub>2</sub>, Fe–ZrO<sub>2</sub>, Ag/ZrO<sub>2</sub> and Ag/Fe–ZrO<sub>2</sub>) were tested in the toluene (C<sub>6</sub>H<sub>5</sub>–CH<sub>3</sub>) oxidation in the presence of water vapor (3.4 vol%). The collected results (C<sub>6</sub>H<sub>5</sub>–CH<sub>3</sub> conversion and CO<sub>2</sub> concentration as temperature reaction function) are shown in Figs. 1A, B.

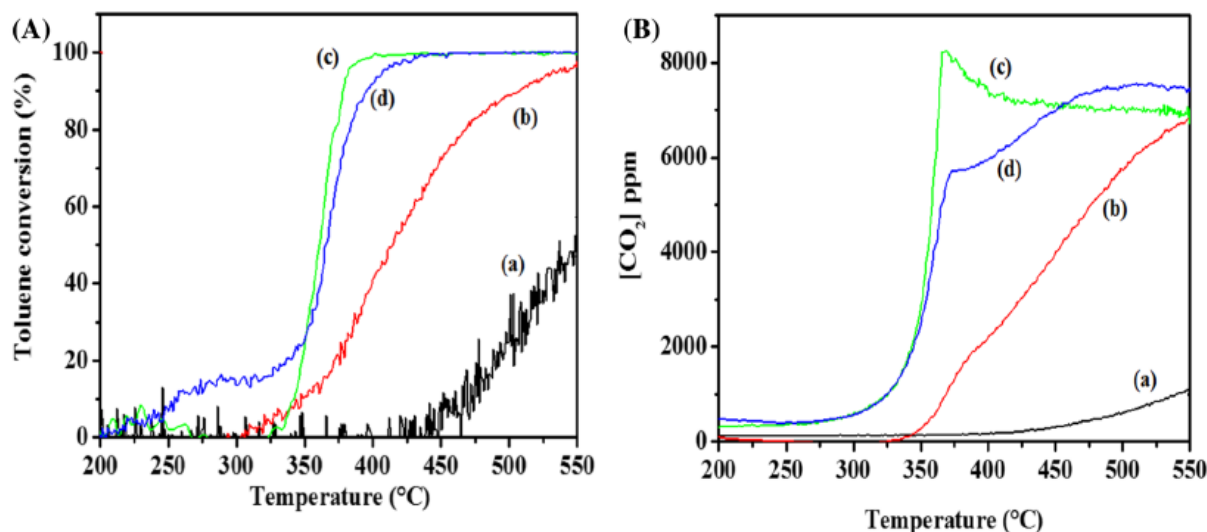


Fig. 1 **A** Toluene conversion and **B** CO<sub>2</sub> concentration (ppm) over (a) ZrO<sub>2</sub>, (b) Fe–ZrO<sub>2</sub>, (c) Ag/ZrO<sub>2</sub>, and (d) Ag/Fe–ZrO<sub>2</sub> samples

The temperatures corresponding to 10%, 50%, and 90% of toluene conversions (denoted as T10, T50, and T90) are used to evaluate and compare the catalytic activities of solids.

It is well established that the mechanism of VOCs oxidation over transition metal oxides follows a Mars–Van Krevelen mechanism, which is known as redox mechanism, involving two successive steps in terms of the cyclic reaction. In the first step, oxygen vacancies on the catalyst surface were reduced as they react with the organic molecules. In the second step, the pre-formed reduced site regenerated immediately through the consumption of gaseous oxygen or the transfer of oxygen atoms from the bulk to the surface [18–20]. Therefore, the oxygen carrier capacities (adsorbed and lattice oxygen species) and reducibility of catalyst determined its reactivity in the oxidation of VOCs [18–21]. Noting that the surface acidity of catalyst also play a key role in the oxidation reaction since it could facilitate both the sorption of VOC at the catalyst surface and the breaking of carbon–carbon bonds which promote the CO<sub>2</sub> production [22].

As it can be seen in Fig. 1, the ZrO<sub>2</sub> support exhibits the lowest C<sub>6</sub>H<sub>5</sub>–CH<sub>3</sub> conversions to CO<sub>2</sub> (a maximum of 50% at 550 °C) due to the low reactivity of its acidic sites in this reaction and the absence of redox ones. However, the addition of iron or silver species significantly enhances the activity for the toluene oxidation. Higher C<sub>6</sub>H<sub>5</sub>–CH<sub>3</sub> conversions to CO<sub>2</sub> are obtained in the 350–550 °C temperature range over Ag/ZrO<sub>2</sub> (near 100%) compared to that observed in the case of the aerogel Fe–ZrO<sub>2</sub> (a maximum of 95% at 550 °C). This result demonstrates that the active sites (most probably acidic and redox

ones) created by silver species are more reactive in the toluene oxidation than those generated by iron ones. The temperatures at which toluene conversion reaches 10%, 50%, and 90%, over Fe–ZrO<sub>2</sub>, Ag/ZrO<sub>2</sub> and Ag/Fe–ZrO<sub>2</sub> catalysts, are indicated in Table 1.

The catalytic activity test demonstrates that Ag/ZrO<sub>2</sub> and Ag/Fe–ZrO<sub>2</sub>, which were found more active than Fe–ZrO<sub>2</sub> (Fig. 1A, B), exhibit approximately a similar oxidation activity at high temperatures (100% of toluene conversion for T > 400 °C). However, the simultaneous presence of Ag and Fe leads to the most active Ag/Fe–ZrO<sub>2</sub> catalyst in the low temperatures range, therefore, T<sub>10</sub> are 349 °C, 341 °C and 250 °C over Fe–ZrO<sub>2</sub>, Ag/ZrO<sub>2</sub> and Ag/Fe–ZrO<sub>2</sub>, respectively. Based on this result, we can suggest the existence of Ag-Fe interactions, which promote the dispersion of silver and iron active species, facilitates the mobility and activation of oxygen, and enhance the reactivity of acidic and redox sites, thereby increasing the low temperature activity of Ag/Fe–ZrO<sub>2</sub> catalyst in the total oxidation of toluene. This is in perfect agreement with the result already obtained by Lu et al. [14] for the non-thermal plasma oxidation of toluene. In fact, the authors have demonstrated that 2%FeO<sub>x</sub>–1%AgO<sub>y</sub>/SBA-15 catalyst exhibits higher stability, toluene removal efficiency and CO<sub>2</sub> selectivity than 3%FeO<sub>x</sub>/SBA-15 system. Their results revealed that silver, existing in the form of Ag particles and Ag<sub>2</sub>O on the catalyst surface, adsorb toluene and promote the production of hydroxygroups, thus improving the reductive activity of FeO<sub>x</sub>. The authors have concluded that the interaction between Ag and Fe species could increase the catalyst activity and consequently improve the performance of the plasma-catalytic degradation of toluene. Meanwhile, Scirè et al. [23] reported that Ag could weaken the Fe–O bond, increase the mobility of the lattice oxygen, and thus improve the VOCs oxidation. By contrast, Rioseco et al. [24] have concluded that no increase in the catalytic activity for the complete combustion of toluene was observed upon low Ag substitution in LaFeO<sub>3</sub> perovskite.

Table 1 Conversions of toluene at different temperatures over the catalysts

Catalyst	T <sub>10</sub> (°C)	T <sub>50</sub> (°C)	T <sub>90</sub> (°C)
ZrO <sub>2</sub>	469	550	–
Fe–ZrO <sub>2</sub>	349	414	506
Ag/ZrO <sub>2</sub>	341	360	377
Ag/Fe–ZrO <sub>2</sub>	~ 250	365	394

Table 2 Catalytic activity of silver-based catalysts in the toluene oxidation

Catalyst	T <sub>10</sub> (°C)	T <sub>50</sub> (°C)	T <sub>90</sub> (°C)	Reference	Catalytic conditions
Ag/Fe–ZrO <sub>2</sub>	~ 250	365	394	This work	GHSV = 60,000 h <sup>-1</sup> , m = 20 mg With 3.4 vol% H <sub>2</sub> O
Ag/γAl <sub>2</sub> O <sub>3</sub>	~ 330	~ 360	~ 380	[25]	GHSV = 15,000 h <sup>-1</sup> , m = 200 mg Without H <sub>2</sub> O
Ag/Cu/Al <sub>2</sub> O <sub>3</sub>	~ 260	~ 280	~ 330	[25]	GHSV = 15,000 h <sup>-1</sup> , m = 200 mg Without H <sub>2</sub> O

With: GHSV = gas hourly space velocity and m = mass of catalyst

It is worthy to note that, the efficiency obtained over the new Ag/Fe–ZrO<sub>2</sub> catalyst in the

low temperature total oxidation of toluene (particularly T10) is better compared to some literature data (Table 2) since the reaction was performed in this work with water vapor (3.4 vol%), at higher gas hourly space velocity (GHSV = 60,000 h<sup>-1</sup>) and with a low amount of catalyst (m = 20 mg).

The results of the N<sub>2</sub> physisorption analysis, given in Table 3, reveal that all the samples exhibit after calcination at 550 °C developed texture (high surface area (SBET ≥ 76 m<sup>2</sup>/g) and total pore volume (VPT ≥ 0.24 cm<sup>3</sup>/g)) demonstrating a good thermal stability of catalysts. Nevertheless, it should be mentioned that a slight decrease of the SBET and VPT accompanied by an increase of the pore diameter of ZrO<sub>2</sub> is observed after Fe and/or Ag addition. This might be attributed, on one hand, to the partial obstruction of some pores of solids by the supported species [26], and on the other hand, to the increase of the crystallite size of zirconia after its modification by iron and/or silver species [27]. Similar results have been obtained by Dastan et al. [27] upon heat treatment of TiO<sub>2</sub> NP's system. The authors have explained the decrease of the surface area and pore volume of this later solid, with the increase of its pore diameter, upon heat treatment, to the increase in the crystallite size and the collapse of pore structure of TiO<sub>2</sub> NP's at higher annealing temperature.

Table 3 Textural properties of samples

Catalyst	Surface area (m <sup>2</sup> /g)	Total pore volume (cm <sup>3</sup> /g)	Average pore diameter ( $\Phi_{\text{pore}}$ , Å)
ZrO <sub>2</sub>	107	0.33	88
Fe-ZrO <sub>2</sub>	93	0.28	92
Ag/ZrO <sub>2</sub>	76	0.24	97
Ag/Fe-ZrO <sub>2</sub>	84	0.26	116

Based on the N<sub>2</sub> adsorption–desorption isotherms and BJH pore size distribution curves of solids (shown in Figs. 2 and 3, respectively) it can be concluded that all the samples are mesoporous systems (isotherms type IV according to the IUPAC classification) with monomodal (case of ZrO<sub>2</sub> and Ag/ZrO<sub>2</sub>: hysteresis loops type H2) or binodal (for Fe-ZrO<sub>2</sub> and Ag/Fe-ZrO<sub>2</sub>: hysteresis loops type H2) porous distribution.

It should be also mentioned that the increase of zirconia pores size after the iron and/or silver addition could indicate the existence of divers interactions between ZrO<sub>2</sub> and the supported species which probably affects the texture of solids as previously suggested for various aerogels catalysts [17].

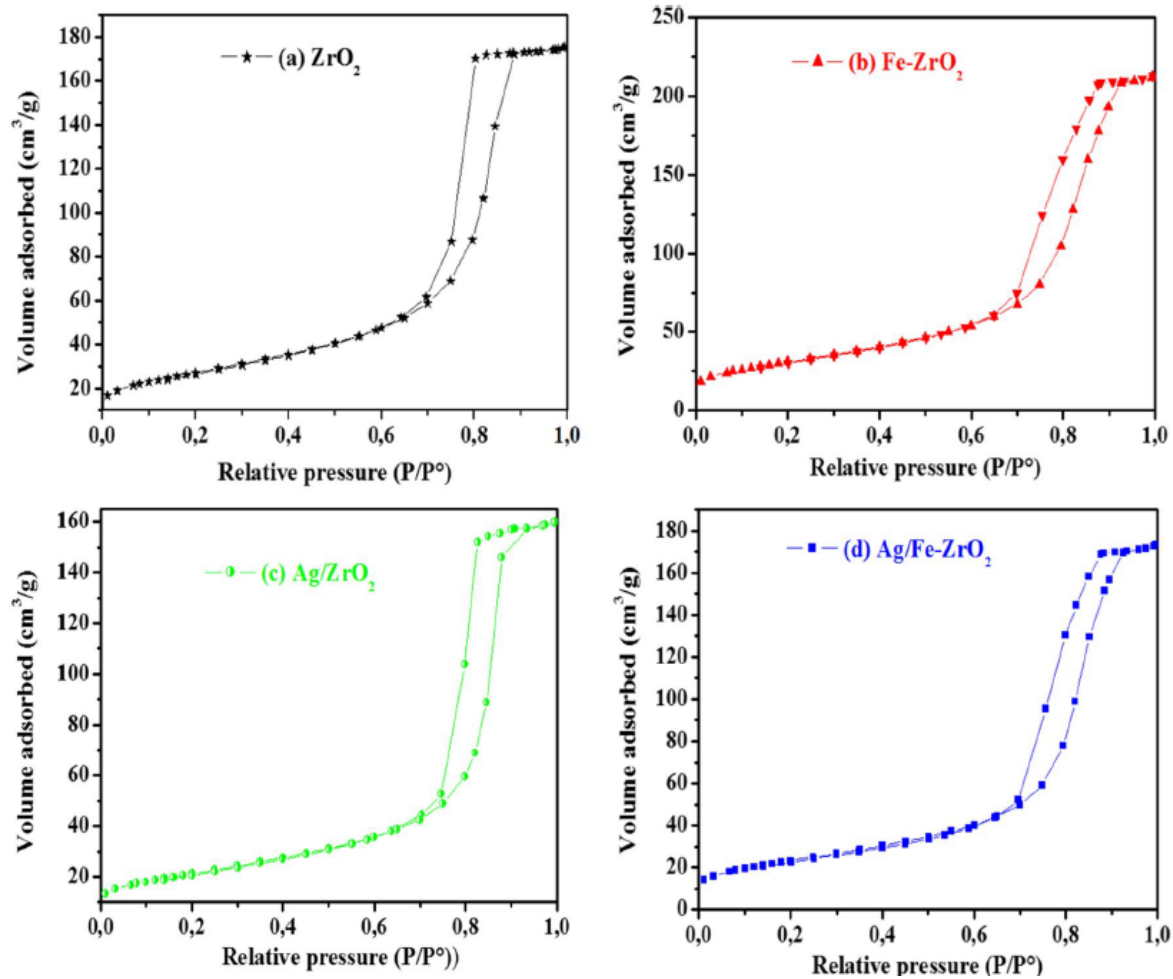


Fig. 2 N<sub>2</sub> adsorption–desorption isotherms of (a) ZrO<sub>2</sub>, (b) Fe-ZrO<sub>2</sub>, (c) Ag/ZrO<sub>2</sub>, and (d) Ag/Fe-ZrO<sub>2</sub> samples



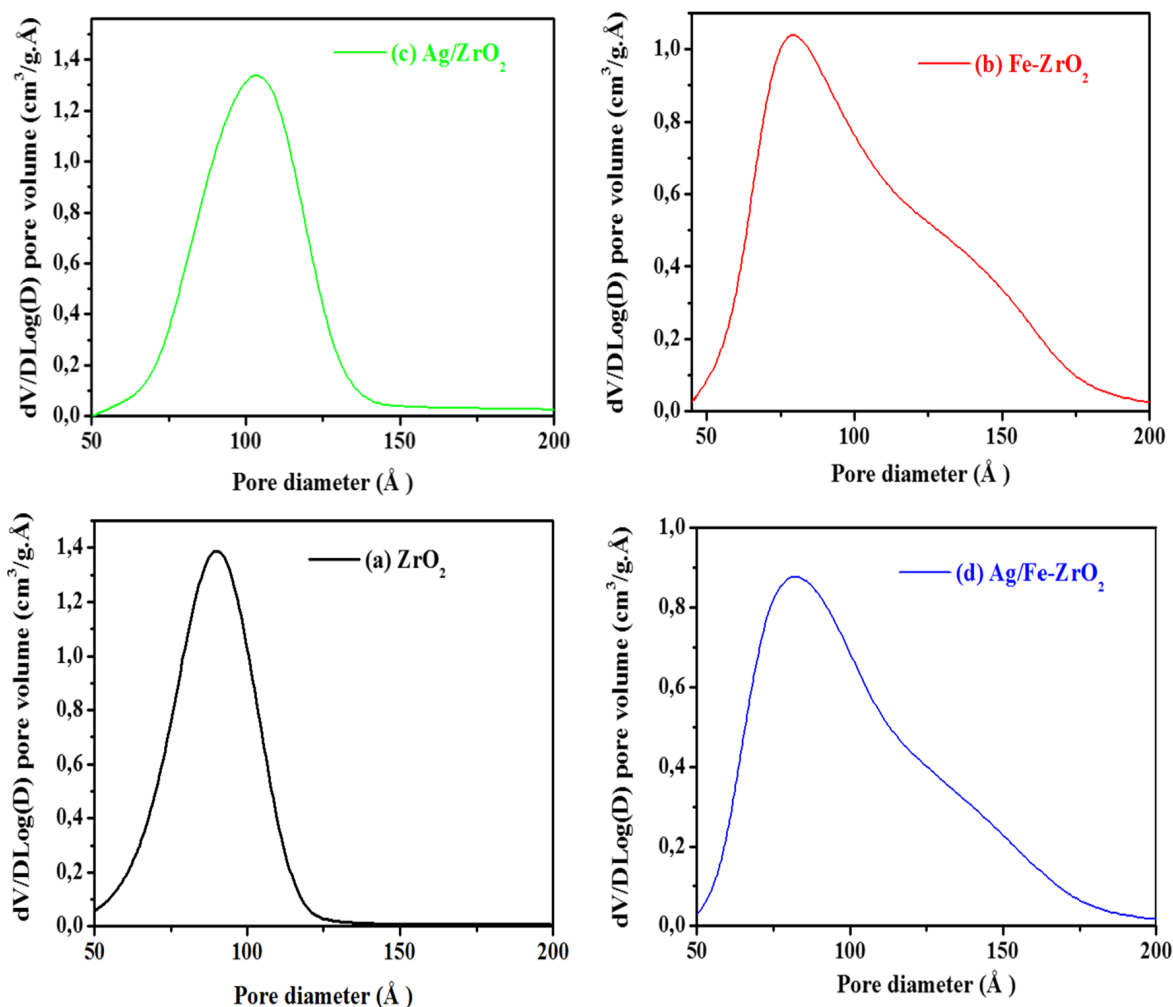


Fig. 3 BJH pore size distribution curves of (a) ZrO<sub>2</sub>, (b) Fe-ZrO<sub>2</sub>, (c) Ag/ZrO<sub>2</sub>, and (d) Ag/Fe-ZrO<sub>2</sub> samples

Figure 4 shows the XRD diffractograms of samples. It is clearly seen that all the solids develop a high crystalline structure of zirconia. Hence, two major diffraction lines corresponding to the monoclinic (m-ZrO<sub>2</sub>) and tetragonal phases (t-ZrO<sub>2</sub>) of ZrO<sub>2</sub> are detected, on the diffractograms of ZrO<sub>2</sub> and Ag/ZrO<sub>2</sub> solids, at  $2\theta = 24.38^\circ$  (110),  $28.26^\circ$  ( $-111$ ),  $31.56^\circ$  (111),  $41.07^\circ$  (102),  $45.21^\circ$  ( $-202$ ),  $54.09^\circ$  (300),  $55.60^\circ$  (130),  $65.68^\circ$  (320) [PDF 89-9066] and  $2\theta = 30.33^\circ$  (101),  $34.67^\circ$  (002),  $50.37^\circ$  (112),  $60.09^\circ$  (211),  $62.57^\circ$  (202) [PDF 79-1769], respectively. Nevertheless, only the typical peaks of the t-ZrO<sub>2</sub> phase are observed in the XRD patterns of Fe-ZrO<sub>2</sub> and Ag/Fe-ZrO<sub>2</sub> catalysts. This suggests the stabilization of the tetragonal phase of zirconia by its interactions with the supported Ag and Fe species.

Markedly, no reflections associated with metallic iron or its oxide phases are found. This implies that Fe species are highly dispersed on ZrO<sub>2</sub> surface. However, a weak diffraction line corresponding to the metallic silver was detected at around  $2\theta = 38.1^\circ$  (111) for Ag/ZrO<sub>2</sub> sample revealing the presence of a trace amount of metallic Ag (PDF 65-2871). This result suggests the existence of Ag-Fe interactions which contribute to the high dispersion of silver species at the catalyst surface.

The crystallites size of pure and modified zirconia is calculated using the Scherrer's formula [28–30] and the obtained values are 10.6, 18, 11.8, and 19.8 nm for ZrO<sub>2</sub>, Fe-ZrO<sub>2</sub>, Ag/ZrO<sub>2</sub>, and Ag/Fe-ZrO<sub>2</sub>, respectively.

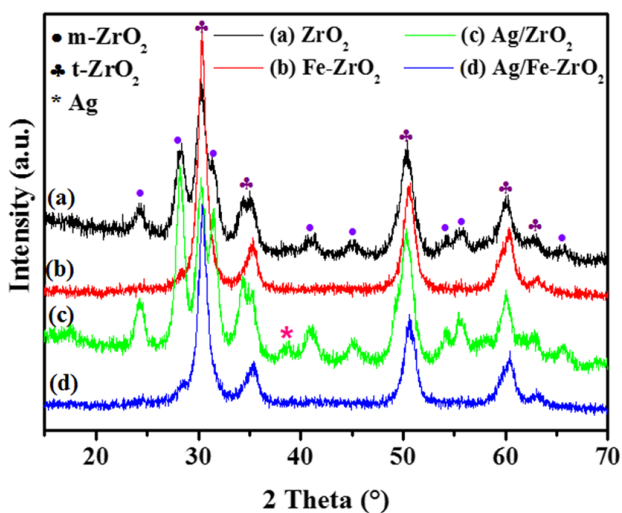


Fig. 4 XRD patterns of (a)  $ZrO_2$ , (b)  $Fe-ZrO_2$ , (c)  $Ag/ZrO_2$ , and (d)  $Ag/Fe-ZrO_2$  samples

Based on this result, it can be concluded that all the samples are characterized by a nanometer size and the addition of Ag and/or Fe contributes to the crystal growth of zirconia.

$H_2$ -temperature-programmed reduction ( $H_2$ -TPR analysis) was performed to study the redox properties of materials and the results are illustrated in Fig. 5.

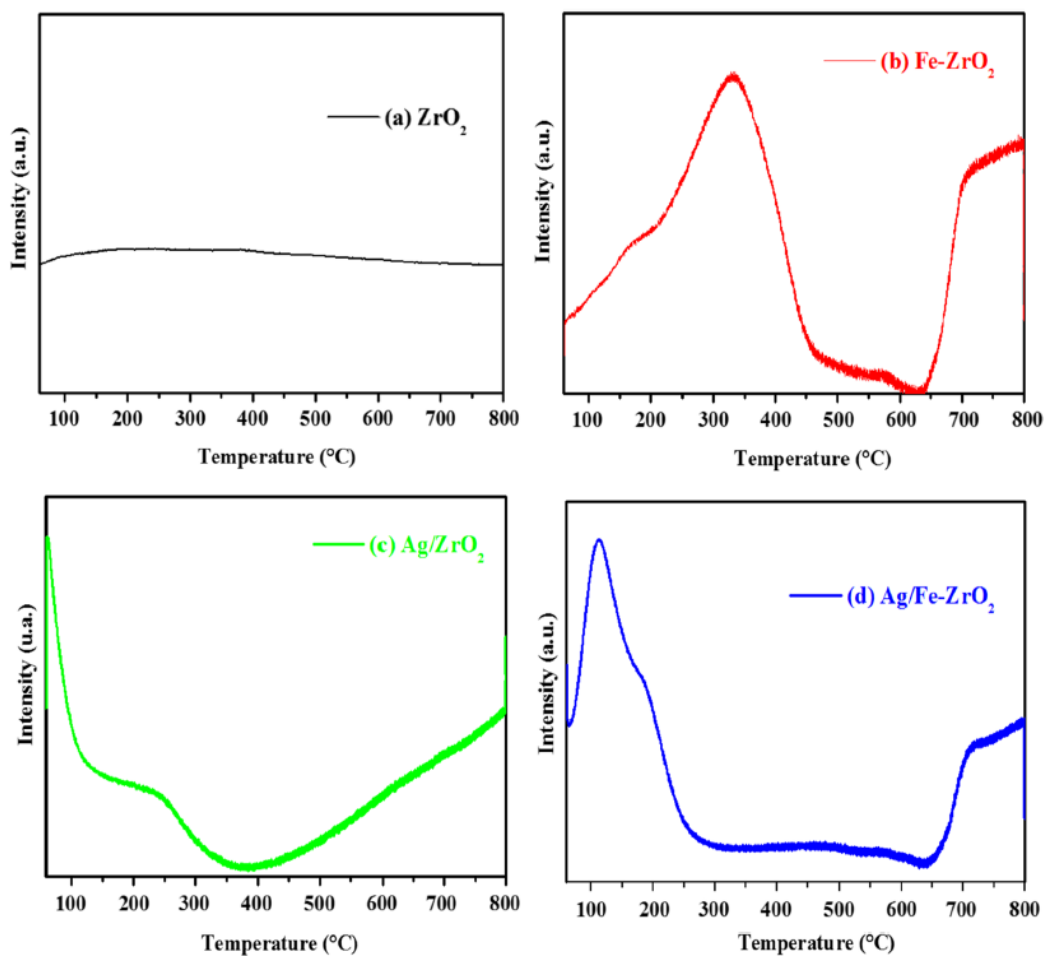


Fig. 5  $H_2$ -TPR of (a)  $ZrO_2$ , (b)  $Fe-ZrO_2$ , (c)  $Ag/ZrO_2$ , and (d)  $Ag/Fe-ZrO_2$  samples

For the ZrO<sub>2</sub> solid, no H<sub>2</sub> consumption peaks are detected indicating that Zr<sup>4+</sup> is a non-reducible cation [31]. For the aerogel Fe–ZrO<sub>2</sub>, two main H<sub>2</sub>-consumption peaks are appeared in the experimental temperature range; the peak at low temperatures (centered at T ≈ 150 °C) could be attributed to the reduction of Fe<sub>2</sub>O<sub>3</sub> to Fe<sub>3</sub>O<sub>4</sub> and the other one, observed at higher temperatures (centered at T ≈ 350 °C), can be associated with the Fe<sub>2</sub>O<sub>3</sub> → Fe<sub>3</sub>O<sub>4</sub> → Fe<sup>0</sup> transformations [32]. Similarly, a new H<sub>2</sub>- consumption peaks are observed at low temperatures (< 300 °C) in the H<sub>2</sub>-TPR profile of Ag/ZrO<sub>2</sub> and Ag/Fe–ZrO<sub>2</sub> catalyst and can be ascribed to the reduction of both silver and iron species [33, 34]. It is noteworthy that after the addition of Ag to Fe–ZrO<sub>2</sub> solid, the reduction peaks of Fe species was shifted to the lower temperatures indicating an enhancement of the iron species reducibility, must probably due to their interactions with silver which is consistent with the XRD results. Similar results, suggesting the improvement of FeO<sub>x</sub> reducibility by silver addition, have been previously obtained by Lu et al. [14] for 2%FeO<sub>x</sub>–1%AgO<sub>y</sub>/SBA-15 system.

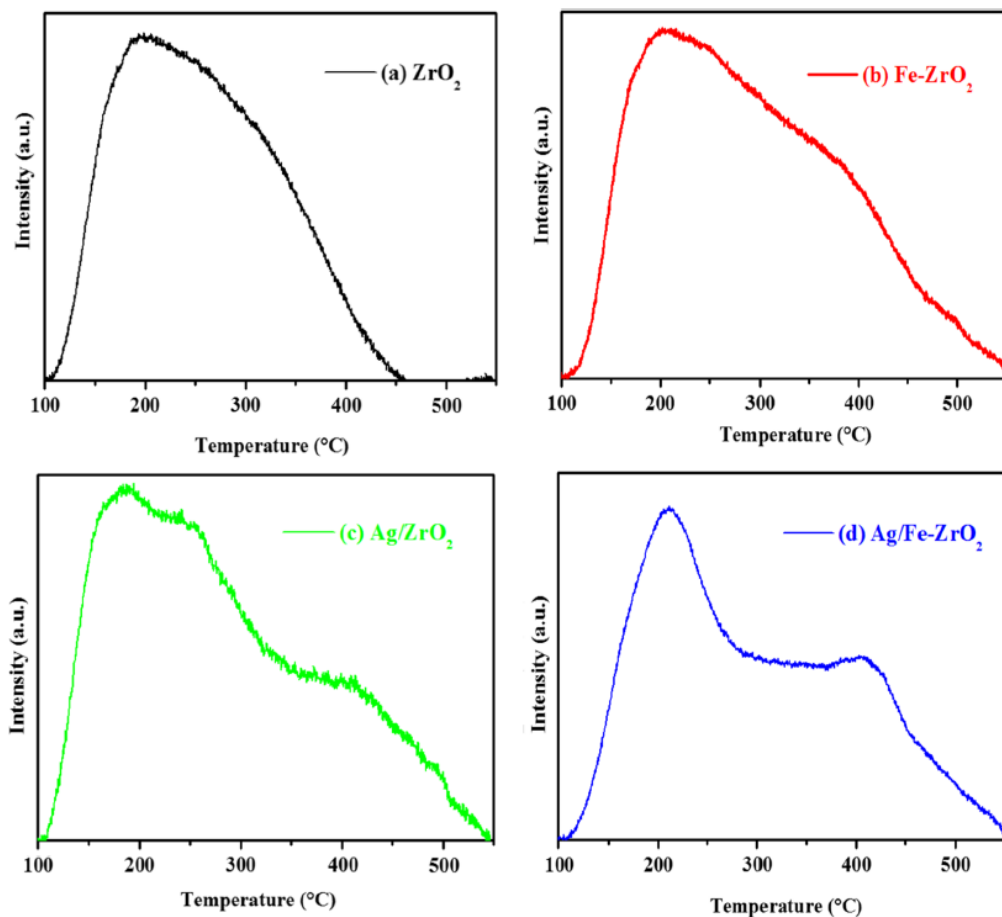


Fig. 6 NH<sub>3</sub>-TPD of (a) ZrO<sub>2</sub>, (b) Fe–ZrO<sub>2</sub>, (c) Ag/ZrO<sub>2</sub>, and (d) Ag/Fe–ZrO<sub>2</sub> samples

The total acidity of solids was evaluated using the temperature-programmed desorption of ammonia (NH<sub>3</sub>-TPD) and the results are presented in Fig. 6. The ZrO<sub>2</sub> and Fe–ZrO<sub>2</sub> aerogel supports show a broad NH<sub>3</sub> desorption peak between 100 and 400 °C corresponding to NH<sub>3</sub> desorbed from weak and medium strong acid sites [35]. The intensity of this former peak is higher for the solid containing Fe compared to that characterizing pure

zirconia. This indicates that the presence of iron increases the total acidity of the support and contributes to the creation of new strong acid sites (NH<sub>3</sub> desorbed at T > 400 °C). The addition of silver affects the total acidity of ZrO<sub>2</sub> and Fe–ZrO<sub>2</sub> solids and leads also to the creating of new strong acid sites (desorption of NH<sub>3</sub> at T > 400 °C), especially, at Ag/Fe–ZrO<sub>2</sub> surface.

## Conclusions

In this work, a highly crystalline and mesoporous ZrO<sub>2</sub>, Fe–ZrO<sub>2</sub>, Ag/ZrO<sub>2</sub>, and Ag/Fe–ZrO<sub>2</sub> catalytic systems were prepared for the total oxidation of toluene in the presence of water vapor. It was shown that the presence of Fe or Ag stabilizes the tetragonal phase of ZrO<sub>2</sub> and leads to the creation of new redox and strong acid sites at zirconia surface. On the other hand, it was revealed that the coexistence of Ag and Fe species promotes both the acidity and reducibility of catalysts and contributes to the formation of more reactive oxygen which is beneficial for the low temperature toluene oxidation. Ag/Fe–ZrO<sub>2</sub> was found to be the most active catalyst in the low temperature total oxidation of toluene (T<sub>10</sub> = 250 °C) and exhibits approximately similar catalytic performances to that obtained over Ag/ZrO<sub>2</sub> at higher temperatures (350–550 °C). Interestingly, 100% toluene conversion to essentially CO<sub>2</sub> is obtained in 400–550 °C temperature range over the new Ag/Fe–ZrO<sub>2</sub> catalyst.

## Compliance with ethical standards

**Conflict of interest** The authors declare that there is no conflict of interest regarding the publication of this article.

## References

1. Kamal MS, Razzak SA, Hossain MM (2016) *Atmos Environ* 140:117–134
2. Yang C, Miao G, Pi YH, Xia Q, Wu JL, Zhong Li Z, Xiao J (2019) *Chem Eng J* 370:1128–1153
3. Zhu L, Shen D, Luo KH (2020) *J Hazard Mater* 389:122102
4. Zhang XD, Shi XY, Chen JF, Yang Y, Lu G (2019) *J Environ Chem Eng* 7:103405
5. Bi F, Zhang XD, Chen JF, Yang Y, Wang YX (2020) *Appl Catal B* 269:118767
6. Zhang XD, Song L, Bi F, Zhang DF, Wang YX, Cui LF (2020) *J Colloid Interface Sci* 571:38–47
7. Zhang CH, Huang H, Li GQ, Wang L, Song L, Li XB (2018) *Catal Today*. <https://doi.org/10.1016/j.catto.2018.03.019>
8. Zhang CH, Wang C, Huang H, Zeng K, Wang Z, Ji HP, Li XB (2019) *Appl Surf Sci* 486:108–120
9. Zeng K, Li XY, Wang C, Wang Z, Guo P, Yu J, Zhang CH, Zhao XS (2020) *J Colloid Interfaces Sci* 572:281–296
10. Zhang CH, Zeng K, Wang C, Liu XH, Wu GL, Wang Z, Wang D (2019) *Ceram Int* 46:6652–6662
11. Bi F, Zhang XD, Xiang S, Wang YY (2020) *J Colloid Interfaces Sci* 573:11–20
12. Torbina VV, Vodyankin AA, Ten VS, Mamontov GV, Salaev MA, Sobolev VI, Vodyankina OV (2018) *Catalysts* 447:2–56
13. Qu Z, Bu Y, Qin Y, Wang Y, Fu Q (2013) *Appl Catal B* 132–133:353–362
14. Lu M, Yang W, Yu C, Liu Q, Ye D (2020) *Aerosol Air Qual Res* 20:193–202
15. Dastan D, Londhe PU, Chaure NB (2014) *J Mater Sci Mater Electron* 25:3473–3479
16. Panahi SL, Dastan D, Chaure NB (2016) *Adv Sci Lett* 22:941–944

17. Arfaoui J, Ghorbel A, Petitto C, Delahay G (2018) *Appl Catal Environ* 224:264–275
18. Susuki M, Tsutsumi K, Takahashi H, Saito Y (1988) *Zeolites* 8:284–291
19. Neyestanaki AK, Kumar N, Linfors LE (1995) *Appl Catal B* 7:95–111
20. Popova M, Szegdi A, Cherkezova-Zheleva Z, Dimitrova A, Mitov I (2010) *Appl Catal A* 381:26–35
21. Antunes AP, Ribeiro MF, Silva JM, Ribeiro FR, Magnoux P, Guisnet M (2001) *Appl Catal B* 33:149–164
22. Windawi H, Wyatt M (1993) *Platinum Met Rev* 37:186–248
23. Sciré S, Minico S, Crisafulli C, Galvagno S (2001) *Catal Commun* 2:229–232
24. Rioseco F, Radovic L, Garacia X, Gordon A, Pecchi G (2010) *J Chil Chem Soc* 55:44–49
25. Kim SC, Moon JH (2011) *J Nanosci Nanotechnol* 1:1660–1663
26. Arfaoui J, Khalfallah-Boudali L, Ghorbel A, Delahay G (2009) *Catal Today* 142:234–238
27. Dastan D, Nandu-Chaure N, Kartha M (2017) *J Mater Sci Mater Electron* 28:7784–7796
28. Jafari A, Alam MH, Dastan D, Ziakhodadadian S, Shi ZC, Garmestani H, Weidenbach AS, Țălu S (2019) *J Mater Sci Mater Electron* 30:21185–21198
29. Jafari A, Tahani K, Dastan D, Asgary S, Shi ZC, Yin XT, Zhou WD, Garmestani H, Țălu S (2020) *Surf Interfaces* 18:100463
30. Dastan D (2017) *Appl Phys A* 123:699. <https://doi.org/10.1007/s00339-017-1309-3>
31. Zheng Y, Zhu X, Wang H, Li KZ, Yang YH, Wei YG (2014) *J Rare Earth* 32(9):842–848
32. Yang F, Huang JL, Odoom-Wubah T, Hong YL, Du MM, Sun DH, Jia LS, Li QB (2015) *Chem Eng J* 269:105–112
33. Tabakova T, Boccuzzi F, Manzoli M, Sobczak JW, Idakiev V, Andreeva D (2006) *Appl Catal A* 298:127–143
34. Zhang J, Li LP, Huang XS, Li GS (2012) *J Mater Chem* 22:10480–10487
35. Cao F, Xiang J, Su S, Wang P, Hu S, Sun L (2015) *Fuel Process Technol* 135:66–72